

1 **Phylogenetic and structural diversity of aromatically dense pili from environmental
2 metagenomes**

3 M. S. Bray^{1,2@}, J. Wu¹, C.C. Padilla^{1#}, F. J. Stewart¹, D. A. Fowle³, C. Henny⁴, R. L. Simister⁵,
4 K. J. Thompson⁵, S. A. Crowe^{2,5}, J. B. Glass^{1, 2*}

5

6 ¹School of Biological Sciences, Georgia Institute of Technology, Atlanta, GA, USA;

7 ²School of Earth and Atmospheric Sciences, Georgia Institute of Technology, Atlanta, GA, USA;

8 ³Department of Geology, University of Kansas, Lawrence, KS, USA;

9 ⁴Research Center for Limnology, Indonesian Institute of Sciences, Cibinong, Indonesia;

10 ⁵Department of Earth, Ocean, & Atmospheric Sciences; Department of Microbiology &

11 Immunology, University of British Columbia, Vancouver, BC, Canada

12

13 *Correspondence to: Jennifer.Glass@eas.gatech.edu

14

15 Running Title: Predicting e-pili

16 [@]Now at: Department of Biological Sciences, San Diego State University, San Diego, CA, USA

17

18 [#]Now at: Dovetail Genomics, LLC, Santa Cruz, CA, USA

19

20 **Originality and Significance.** Electroactive pili (e-pili) are used by microorganisms to respire
21 solid metals in their environment through extracellular electron transfer. Thus, e-pili enable
22 microbes to occupy specific environmental niches. Additionally, e-pili have important potential
23 for biotechnological applications. Currently the repertoire of known e-pili is small, and their
24 environmental distribution is largely unknown. Using sequence analysis, we identified numerous
25 genes encoding putative e-pili from diverse anoxic, metal-rich ecosystems. Our results expand
26 the diversity of putative e-pili in environments where metal oxides may be important electron
27 acceptors for microbial respiration.

28

29 **Summary.** Electroactive type IV pili, or e-pili, are used by some microbial species for
30 extracellular electron transfer. Recent studies suggest that e-pili may be more phylogenetically
31 and structurally diverse than previously assumed. Here, we used updated aromatic density
32 thresholds ($\geq 9.8\%$ aromatic amino acids, ≤ 22 -aa aromatic gaps, and aromatic amino acids at
33 residues 1, 24, 27, 50 and/or 51, and 32 and/or 57) to search for putative e-pilin genes in
34 metagenomes from diverse ecosystems with active microbial metal cycling. Environmental
35 putative e-pilins were diverse in length and phylogeny, and included truncated e-pilins in
36 *Geobacter* spp., as well as longer putative e-pilins in Fe(II)-oxidizing *Betaproteobacteria* and
37 *Zetaproteobacteria*.

38 **Introduction.** Electroactive microbes transport electrons through cell membranes into the
39 extracellular environment (Sydow et al., 2014; Koch and Harnisch, 2016; Logan et al., 2019).
40 These microbes play important roles in biogeochemical cycles in soils and sediments,
41 bioremediation of toxic metals, and energy generation in microbial fuel cells (Lovley, 1991;
42 Lovley and Coates, 1997; Logan, 2009; Lovley, 2011; Mahadevan et al., 2011). Electroactive
43 *Delta*proteobacteria in the genus *Geobacter* (order *Desulfuromonadales*) perform long-range
44 extracellular electron transfer (EET) through electroactive pili (e-pili), composed of e-pilin
45 structural subunits (Lovley, 2017; Lovley and Walker, 2019). *Geobacter* use e-pili for Fe(III)
46 respiration, direct interspecies electron transfer (DIET), and growth on anodes (Reguera et al.,
47 2005; Reguera et al., 2006; Rotaru et al., 2014).

48 *Geobacter* e-pili belong to the larger family of type IV-a pilins (T4aPs), which are
49 broadly distributed in Bacteria and Archaea (Imam et al., 2011; Giltner et al., 2012; Berry and
50 Pelicic, 2015). T4aPs have evolved to perform diverse cellular functions, including twitching
51 motility, attachment, and genetic transformation. Most characterized *Geobacter* e-pilins are
52 truncated versions of canonical T4aPs (Holmes et al., 2016). Type II (or “pseudopilin”) proteins
53 are structurally similar to, but phylogenetically distinct from T4aPs, and assemble into type II
54 secretion (T2S) systems instead of pili (Ayers et al., 2010).

55 Aromatic amino acid density seems to be essential for efficient electron transport in e-pili
56 (Vargas et al., 2013; Liu et al., 2014; Liu et al., 2019). The close packing of aromatic residues
57 within the pilus likely facilitates EET (Reardon and Mueller, 2013; Feliciano et al., 2015;
58 Lovley, 2017). In particular, Phe1, Tyr24, and Tyr27 are key residues (Xiao et al., 2016), and
59 Tyr32, Phe51 and Tyr57 also play important roles (Liu et al., 2019). The most conductive e-pilus
60 measured to date is that of *Geobacter metallireducens*, which contains pilins that are 59 aa in

61 mature length (after signal peptide sequence removal at the prepilin cleavage site) and comprised
62 of 15.3% aromatics and no aromatic-free gaps >22 aa (**Table S1**). The *G. metallireducens* e-pilus
63 is 5000 times more conductive than the *Geobacter sulfurreducens* e-pilus, which has pilins
64 which are 61 aa in mature length and comprised of 9.8% aromatics and no aromatic-free gaps
65 >22 aa (Tan et al., 2017). The *G. sulfurreducens* e-pilus is 100 times more conductive than the
66 *Geobacter uraniireducens* pilus, which contains much longer pilins (193 aa), 9.1% aromatics,
67 and a 53 aa aromatic-free gap (Tan et al., 2016). Non-electroactive T4aPs are thought to be
68 incapable of electroactivity due to insufficient aromatic residue packing (Feliciano et al., 2015;
69 Malvankar et al., 2015; Kolappan et al., 2016). To our knowledge, the most aromatic-rich
70 predicted e-pilus belongs to *Desulfobacula phenolica* (16.9%; Holmes et al., 2016).

71 Multiheme cytochromes (MHCs) are also involved in EET. Outer membrane MHCs
72 move electrons from the periplasm into the extracellular environment (Aklujkar et al., 2013). The
73 hexaheme OmcS can localize with *Geobacter* e-pili (Leang et al., 2010; Vargas et al., 2013; Liu
74 et al., 2014). Conductive filaments comprised solely of OmcS were recovered from outer-
75 membrane preparations of *G. sulfurreducens* grown in microbial fuel cells (Filman et al., 2019;
76 Wang et al., 2019), but substantial evidence suggests that e-pilins in wild-type *Geobacter*
77 cultures are comprised of PilA (Lovley and Walker, 2019).

78 Recently, the phylogenetic and structural diversity of e-pili has expanded beyond
79 *Geobacter* spp. with the discovery of strongly conductive pili in clades outside of *Geobacter*
80 genera, including *Syntrophus aciditrophicus* (*Delta*proteobacteria/*Syntrophobacteriales*),
81 *Desulfurivibrio alkaliphilus* (*Delta*proteobacteria/*Desulfobacteriales*), *Calditerrivibrio*
82 *nitroreducens* (*Deferribacteres*), and the archaeon *Methanospirillum hungatei*
83 (*Euryarchaeota/Methanomicrobiales*) (Walker et al., 2018; Walker et al., 2019a; Walker et al.,

84 2019b) (**Table 1**). Pilin genes in these four microbes are much longer (110-182 aa) than in
85 *Geobacter* spp., but have similar aromaticity (11-13%) and similar maximum aromatic-free gaps
86 (22-35 aa). Pili from *Desulfovibrio auxilii*, *Shewanella oneidensis*, and *Pseudomonas*
87 *aeruginosa* with minimal conductance have lower aromaticity (5.6-6.8%) and larger aromatic-
88 free gaps (42-52 aa; Reguera et al., 2005; Liu et al., 2014; Walker et al., 2018). Therefore, it
89 seems that aromatic density, defined here as percentage of aromatic amino acids and spacing of
90 aromatic residues in the pilin sequence, is the key factor for identifying putative e-pilins based on
91 sequence similarity (Walker et al., 2019a). In this study, we searched metagenomes from metal-
92 rich environments and enrichment cultures for putative e-pilins based on aromatic density and
93 spacing.

94

95 **Results**

96 ***Aromatic density and spacing distinguishes e-pilins from non-conductive T4aPs.*** We obtained
97 published sequences for seven biochemically confirmed e-pilins, four non-conductive pilins
98 (**Table S1**), and 35 functionally verified attachment/motility/competence T4aPs (**Table S2**).
99 Biochemically confirmed e-pilins had mature lengths of 59-182 aa, 9.8-16.9% aromatics, and
100 maximum aromatic-free gaps of 22-35 aa (**Figure 1; Table S1**). Pilins implicated in functions
101 other than long-range EET had 93-208 aa mature lengths, 3.5-11.0% aromatics, and 22-75 aa
102 aromatic-free gaps (**Figure 1; Table S2**). Sequence alignments showed that all bacterial e-pilins
103 contained Phe1, Tyr24, Tyr27, and Tyr/Phe51. Most also contained an aromatic amino acid (Tyr
104 or Phe) at residues 32, 50, and 57. Therefore, we used $\geq 9.8\%$ aromatics, ≤ 22 -aa aromatic-free
105 gap, and the presence of aromatic amino acids at residues 1, 24, 27, 50 and/or 51, and 32 and/or
106 57 as a conservative threshold for predicting putative e-pilins from metagenomes, consistent with

107 thresholds established by Walker et al. (2019a). Using these thresholds, two T4aPs in **Table S2**
108 were predicted to be conductive: *G. sulfurreducens* OxpG, which forms a T2S system required
109 for reduction of insoluble Fe(III) (Mehta et al., 2006), and *Dichelobacter nodosus* PilE, which is
110 required for extracellular protease secretion and competence (Han et al., 2007).

111 ***Putative e-pilins are present in ferruginous environments.*** We used the *G.*
112 *sulfurreducens* e-pilin to query metagenomic contigs or metagenome-assembled genomes
113 (MAGs) from environments with conditions amenable to metal respiration. We included
114 metagenomes from ferruginous sediments from two lakes, Lake Matano and Lake Towuti, in the
115 Malili Lakes system on Sulawesi, Indonesia, and the ferruginous water column from Kabuno
116 Bay, Lake Kivu, Democratic Republic of Congo. These permanently stratified tropical lakes host
117 one of the largest ferruginous environments on modern Earth with abundant iron-cycling
118 microbes likely capable of EET (Crowe et al., 2007; Vuillemin et al., 2016). Other environments
119 included deep groundwaters from Sweden (Asop Hard Rock), Japan (Horonobe Underground
120 Laboratory), USA (Rifle, Colorado), and the North Atlantic (North Pond marine aquifer). We
121 also included putative e-pilins from year-long laboratory incubations inoculated with Lake
122 Matano sediment amended with Fe(III) or Mn(III) (see **Experimental Procedures**).

123 We screened the retrieved amino acid sequences for T4Ps using Pilfind (Imam et al.,
124 2011), and the aromatic density thresholds established above ($\geq 9.8\%$ aromatic amino acids, $\leq 22\%$
125 aa aromatic gaps, and aromatic amino acids at residues 1, 24, 27, 50 and/or 51, and 32 and/or
126 57). After partial sequences were removed, we recovered putative e-pilins ranging from 58 to
127 162 aa mature length with 9.8-15.5% aromatic density (**Table S3; Supplemental Data File**).

128 ***Widening the phylogenetic diversity of putative e-pilins.*** To determine the phylogenetic
129 diversity of environmental e-pilins, we constructed a maximum likelihood tree from an

130 alignment of the T4aP amino acid sequences described above, as well as additional predicted
131 *Delta*proteobacteria e-pilins from cultured species (Holmes et al, 2016; Walker et al., 2018a)
132 and BLAST searches (**Figure 2**). *M. hungatei* e-pilin was used as the outgroup. The T4aP
133 phylogeny was broadly consistent with previous findings (Holmes et al., 2016; Walker et al.,
134 2018). All truncated e-pilins and all confirmed bacterial e-pilins clustered with
135 *Delta*proteobacteria. Non-conductive *Gamma*proteobacteria pilins and T2S pseudopilins fell on
136 separate branches. Truncated *Desulfuromonadales* e-pilins (~60 aa) formed their own branch
137 within the *Delta*proteobacteria cluster. Other branches on the *Delta*proteobacteria cluster
138 contained recently discovered e-pilins from *Desulfobacterales*, *Deferribacteres*, and
139 *Syntrophobacterales*. Roughly half of environmental putative e-pilins clustered with
140 *Delta*proteobacteria, including two putative e-pilins from native Lake Matano sediment and six
141 putative e-pilins from >1 year anoxic incubations of Lake Matano sediments with Fe(III) oxides
142 (**Table S3; Supplemental Data File**). Putative e-pilins from marine *Zet*proteobacteria
143 (*Mariprofundus micogutta* and two MAGs from the North Pond marine subsurface aquifer) and
144 *Nitrospinae* (Crystal Geyser, Utah, USA) also clustered with *Delta*proteobacteria e-pilins.

145 Approximately half of environmental putative e-pilins fell outside the
146 *Delta*proteobacteria cluster on the T4aP phylogeny (**Figure 2**). Eight unique putative e-pilin
147 sequences (found 29 times in Kabuno Bay metagenomes), and one e-pilin from McNutt Creek
148 (Georgia, USA), formed a distinct phylogenetic cluster with *pilE* genes from cultured
149 *Beta*proteobacteria (*Gallionella*, *Leptothrix*, *Methylotenera*, *Sulfuricella*, *Thauera*, and
150 *Dechloromonas*), *Gallionellales* MAGs from groundwater, and *Rhodocyclales* MAG from Lake
151 Matano enrichment cultures (311FMe.001; NCBI genome accession VAUH01000000).
152 *Beta*proteobacteria PilE sequences in this clade contained 10.1-13.5% aromatics, ≤22-aa

153 aromatic-free gaps, and key aromatic residues at positions 1, 24, 27, 50, 51, and 57. In all cases,
154 putative *Betaproteobacteria pilE* genes were followed by *fimT-pilVWXYI*, which encode minor
155 pilin assembly proteins (Nguyen et al., 2015).

156 Several putative environmental e-pilins clustered with non-conductive pilins from
157 *Deltaproteobacteria*, *Gammaproteobacteria*, and *Firmicutes*. These included putative e-pilins in
158 MAGs belonging to the candidate phylum *Dependentiae* (formerly TM6) from Rifle
159 groundwater, *Alteromonas NORP73* from North Pond marine subsurface aquifer,
160 *Gammaproteobacteria* HGW15 from Horonobe Underground Laboratory, and *Proteobacteria*
161 CG-11 from Crystal Geyser. The *G. sulfurreducens* OxpG, two sequences from Lake Matano
162 enrichment cultures, and *Omnitrophica* sequences from Crystal Geyser were located on the same
163 branch as the outgroup. *Omnitrophica* have been implicated in anaerobic respiration with metals
164 (Hernsdorf et al., 2017) or sulfite (Anantharaman et al., 2018). To assess potential capacity for
165 metal reduction, we searched MAGs that contained putative e-pilins for outer
166 membrane/extracellular MHCs. Notably, the *Omnitrophica* MAG contained ten putative MHCs
167 located adjacent to each other in the genome, three of which were predicted to be extracellular or
168 outer-membrane MHCs, each with 11 or 13 hemes (**Figure S1**).

169
170 **Discussion.** We recovered genes that meet *in silico* requirements for conductivity based on
171 aromatic density and spacing both inside and outside of the well-established *Deltaproteobacteria*
172 cluster. Our phylogenetic analyses suggest that the *Deltaproteobacteria* e-pilin genes have
173 undergone more extensive horizontal gene transfer (HGT) than previously known. Our results
174 suggest that truncated e-pilins are limited to the *Deltaproteobacteria* cluster, whereas predicted
175 e-pilins outside of *Deltaproteobacteria* were full-length. In addition to their previously

176 recognized HGT to several *Deferribacteres* species (Holmes et al, 2016; Walker et al., 2018a),
177 we found putative e-pilins that clustered with *Deltaproteobacteria* in MAGs from *Nitrospinae*
178 and *Zetaproteobacteria*. *Nitrospinae* are chemoautotrophic nitrite oxidizers that have not, to our
179 knowledge, previously been implicated in EET. *Zetaproteobacteria*, the dominant marine Fe(II)
180 oxidizers, were known to possess *pilA* genes, but the gene products were previously classified as
181 non-conductive because they are >100 aa in length (He et al., 2017). Given the recent discovery
182 of conductive e-pili with >100 aa (Walker et al., 2018), the possible occurrence of e-pilins in
183 *Zetaproteobacteria* such as *Mariprofundus micogutta* needs to be re-evaluated.

184 Outside of the *Deltaproteobacteria* cluster, several putative e-pilin genes clustered with
185 non-conductive *Gammaproteobacteria* pilin. These included *Alteromonas NORP73* from the
186 North Pond marine subsurface aquifer and *Gammaproteobacteria HGW15* from Horonobe
187 Underground Laboratory. *Alteromonas* are known to reduce Fe(III) and form electroactive
188 biofilms (Vandecandelaere et al., 2008), but have not previously, to our knowledge, been found
189 to possess e-pilins. The findings suggest that non-conductive full-length pilins may be capable of
190 evolving conductive properties, although this awaits experimental validation.

191 Putative e-pilins were also found associated with clades not previously known to possess
192 e-pili. Kabuno Bay metagenomes contained abundant e-pilin sequences most similar to those
193 found in metabolically diverse *Betaproteobacteria* genera, including *Gallionella*, *Leptothrix*,
194 *Methylotenera*, *Sulfuricella*, *Thauera*, and *Dechloromonas*. These putative e-pilin genes were
195 classified as *pilE* and were followed by genes involved in minor pilus assembly. Putative
196 *Betaproteobacteria* e-pili genes were also found in other groundwater MAGs, including Crystal
197 Geyser, where *Gallionellaceae* are among the most abundant bacteria (Probst et al., 2018).

198 While the aromatically dense pilins in this study met the bioinformatic thresholds for e-
199 pili, it is possible that they are used for another function, such as DIET (Holmes et al., 2017;
200 Walker et al., 2019a) or cellular detection of solid surfaces via electrical communication (Lovley,
201 2017). Evaluation of the conductivity of the putative e-pilins awaits testing by genetic
202 complementation of $\Delta pilA$ in *G. sulfurreducens*, as in Walker et al. (2018).

203 **Conclusions.** This study identified putative e-pilins in the environment using aromatic
204 density and gaps as the predictive tool, building off of previous studies that established the
205 conductivity of longer PilA proteins (Walker et al., 2018). The sequences we recovered suggest
206 that e-pilins are both phylogenetically and structurally diverse. We conclude that e-pili may be
207 composed of pilin monomers of a variety of lengths and aromatic densities, and that diverse
208 bacteria, including Fe(II)-oxidizing *Betaproteobacteria* and *Zetaproteobacteria*, may use e-pili
209 for EET or possibly other unknown functions.

210 **Acknowledgements.** This research was funded by NASA Exobiology grant
211 NNX14AJ87G with support from the NASA Astrobiology Institute (NNA15BB03A). SAC,
212 RLS, and KTJ were supported through NSERC Discovery grant 0487, CFI projects 229652 and
213 36071, and the Canada Research Chairs program. We thank Bianca Costa, Miles Mobley,
214 Benjamin Reed, and Johnny Striepen for assistance with laboratory incubations, and Sean Elliott
215 and Betül Kaçar for helpful discussions.

216 **Experimental Procedures**

217

218 **Sampling and enrichment of Lake Matano Sediment.** Two sediment cores were obtained
219 from 590 m water depth in Lake Matano, Sulawesi Island, Indonesia in May 2010 (2°28'S,
220 121°20'E, *in situ* sediment temperature ~27°C) and stored under anoxic conditions. The
221 sediments were mixed with anoxic freshwater media in a 1:5 ratio in an anoxic chamber and
222 dispensed in stoppered serum bottles, as in Bray et al. (2017). Cultures were amended first with
223 goethite and later with ferrihydrite. They were incubated for 490 days at 30°C, with multiple
224 transfers, each time diluting the original sediment with freshwater media. Sediment had been
225 diluted over 1000-fold by the time DNA was extracted for sequencing. Details on metagenomes
226 from 395-day anoxic enrichments of Lake Matano sediment incubated with Mn(III)
227 pyrophosphate are reported in a separate publication (Szeinbaum et al., 2019).

228

229 **DNA extraction and metagenome sequencing, assembly, binning and annotation.**
230 Community DNA from Lake Matano sediment enrichments was extracted from 2□g samples
231 and purified using a PowerSoil Isolation Kit and UltraClean® 15 Purification Kit (formerly MO
232 BIO Laboratories, now Qiagen, Carlsbad, CA, USA) following the manufacturer's protocol.
233 Indexed libraries were created from purified community DNA using the NexteraXT DNA
234 Sample Prep kit (Illumina, San Diego, CA, USA) following manufacturer instructions. Libraries
235 were pooled and sequenced on two runs of an Illumina MiSeq using a 500 cycle (paired end 250
236 x 250 bp) kit. Illumina reads were quality trimmed using Trim Galore!
237 (http://www.bioinformatics.babraham.ac.uk/projects/trim_galore/) with a quality score and
238 minimum length cutoff of Q25 and 100 bp, respectively, and merged with FLASH with the
239 shortest overlap of 25 bp. Barcoded sequences were de-multiplexed, trimmed (length cutoff 100
240 bp), and filtered to remove low quality reads (average Phred score <25) using Trim Galore!.
241 Forward and reverse reads were assembled using SPAdes (Nurk et al., 2013) with the 'meta'
242 option. The number of contigs, contig length, GC content, N50, and L50 assembly statistics
243 were calculated with metaQUAST (Mikheenko et al., 2015). Raw sequence reads, and all
244 genomic bins were deposited in NCBI under the accession number [PRJNA505658](https://www.ncbi.nlm.nih.gov/PRJNA505658).

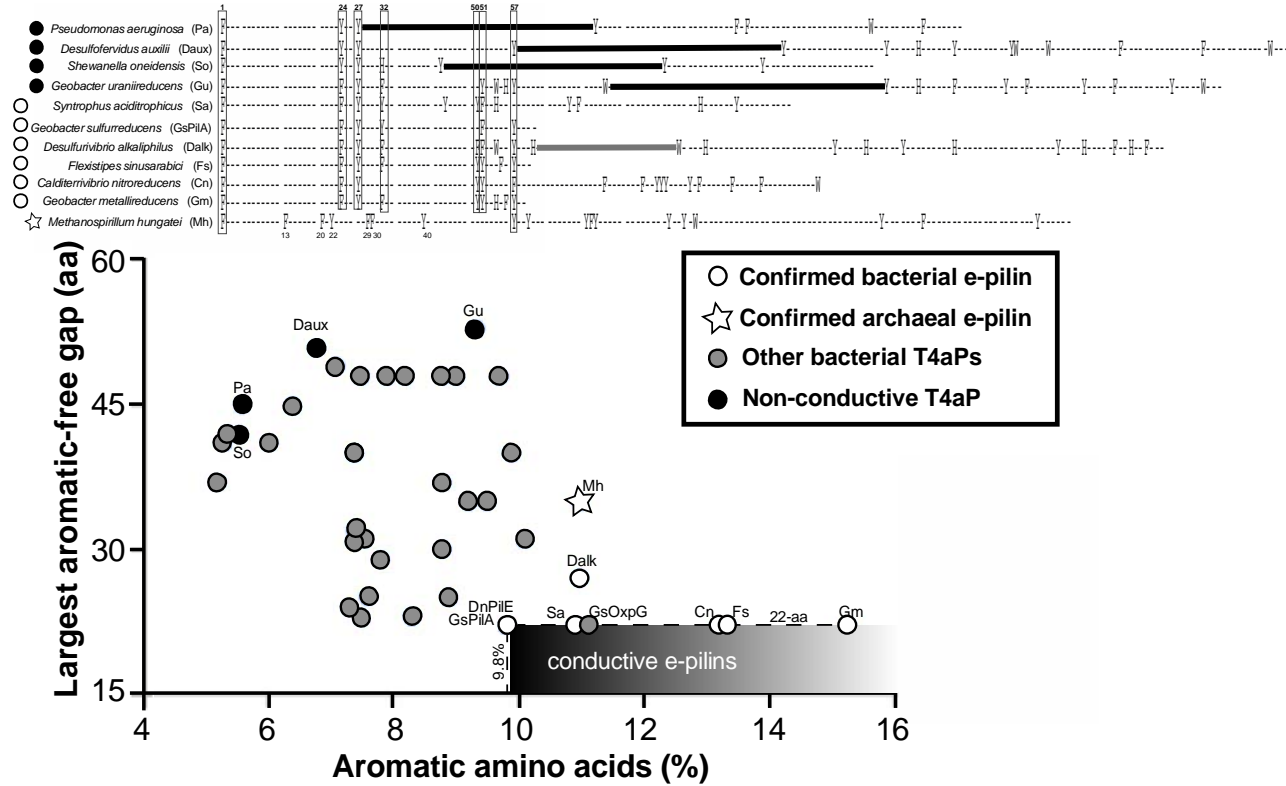
245

246 **E-pilin identification from microbial metagenomes.** Environmental metagenomes and MAGs
247 were downloaded from IMG-JGI and NCBI (see **Table 1** for taxon object IDs). For all
248 metagenomes, Prodigal (Hyatt et al., 2010) was used to predict genes from contig files and write
249 them to amino acid fasta files. Amino acid sequences from MAGs were downloaded directly
250 from NCBI. Predicted protein files were then used as databases for protein BLAST, using the *G.*
251 *sulfurreducens* PilA protein as query. Hits with a bit score greater than 55 were pulled from the
252 databases. These recovered sequences were then further verified as T4P using Pilfind
253 (<http://signalfind.org/pilfind.html>), a web tool that identifies type IV pilin signal sequences
254 (Imam et al., 2011). Pilin amino acid sequences were then run through a python script that
255 calculated the mature pilin length, percent aromatic amino acids, and aromatic free gaps
256 (<https://github.com/GlassLabGT/Python-scripts>). Partial genes were retained if truncated on the
257 N-terminus before the signal peptide and removed if truncated on the C-terminus. Remaining
258 sequences were manually screened for the presence of aromatic amino acids at residues 1, 24, 27,
259 50 and/or 51, and 32 and/or 57.

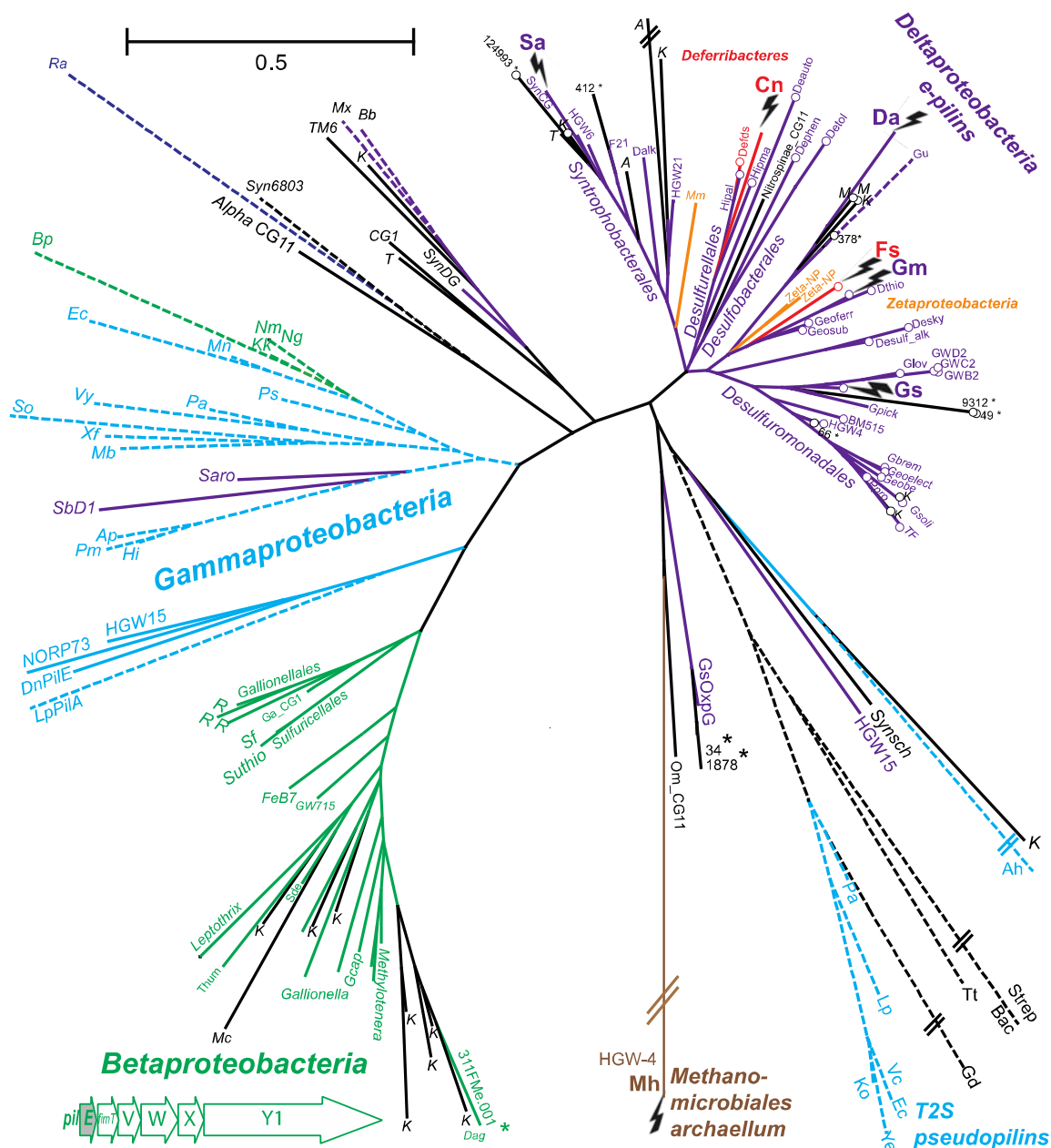
260

261 **Pilin multiple sequence alignment and phylogenetic analysis.** Identified pilin amino acid
262 sequences were aligned using MUSCLE and a maximum likelihood tree was constructed using
263 MEGA. The alignment is provided as **Supplemental Material**. The evolutionary history was
264 inferred by using the Maximum Likelihood method based on the JTT matrix-based model (Jones
265 et al., 1992). Archaeal pili from *M. hungatei* and two other *Methanomicrobiales* were used for
266 the outgroup. The tree with the highest log likelihood is shown. Initial tree(s) for the heuristic
267 search were obtained automatically by applying Neighbor-Join and BioNJ algorithms to a matrix
268 of pairwise distances estimated using a JTT model, and then selecting the topology with superior
269 log likelihood value. There were 52 positions total in the final dataset. Evolutionary analyses
270 were conducted in MEGA7 (Kumar et al., 2016).

271
272 **Multiheme cytochrome analysis.** Groundwater MAGs in which we identified aromatically
273 dense pilins were further probed for the presence of multiheme cytochrome proteins. Amino
274 acids files were run through the “cytochrome_stats.py” described in (Badalamenti et al., 2016)
275 available at <https://github.com/bondlab/scriptsm>, which identifies proteins with 3 or more
276 cytochrome-binding motifs (Cxx(x)CH).



277
278 **Figure 1. Basis for distinguishing e-pilins from other pilins.** *Top:* Alignment showing the
279 location of aromatic residues in each pilin tested for conductivity in previous studies (**Table S1**).
280 Dark horizontal lines indicate 42-53 aa aromatic-free gaps in non-conductive pilins. Conserved
281 N-terminal aromatic residues in bacterial e-pilins are indicated by vertical boxes. All bacterial e-
282 pilins contained F-1, Y-24, Y-27, Y/F-51, Y/F-50 and/or Y/F-57, and H/Y/F-32 and/or Y/F-57.
283 The only N-terminal residues shared by archaeal and bacterial e-pilins were F-1 and Y-57.
284 *Bottom:* Relationship between gap size and percentage of aromatic amino acids in the mature
285 pilin peptide for four types of pilins, which was used to establish conservative criteria for
286 identifying putative e-pilins in environmental metagenomes. Therefore, we used $\geq 9.8\%$
287 aromatics and $\leq 22\text{-aa}$ aromatic-free gap (boxed area labeled “conductive e-pilins”), and the
288 presence of aromatic amino acids at residues as a conservative threshold for predicting putative
289 e-pilins from metagenomes, consistent with thresholds established by Walker et al. (2019a).
290 Additional information about each pilin is in **Tables S1 and S2**.
291



292
293
294
295
296
297
298
299
300
301

Figure 2. Maximum likelihood phylogenetic tree of pilin sequences. *Methanomicrobiales* archaellum was used as the outgroup. Asterisks indicate putative e-pilins from enrichment cultures. Dashed lines indicate sequences that do not meet the criteria for e-pili. Double lines indicate that the branch length was shortened to fit inside the figure boundaries. The gene order for *Betaproteobacteria* putative e-pilins (*pilE*) is shown. See **Supplemental Data File** for details on each sequence and full names of species. **Table S2** provides characteristics of type IV pilins and Type II secretion (T2S) pseudopilins involved in functions other than EET. Environmental abbreviations: A:Asop, CG:Crystal Geyser, K:Kabuno, M:Matano, Mc:McNutt, R:Rifle, T:Towuti.

302 **References**

303 Aklujkar, M., Coppi, M., Leang, C., Kim, B., Chavan, M., Perpetua, L., Giloteaux, L., Liu, A., and
304 Holmes, D. (2013) Proteins involved in electron transfer to Fe(III) and Mn(IV) oxides by *Geobacter*
305 *sulfurreducens* and *Geobacter uraniireducens*. *Microbiology* **159**: 515-535.

306 Anantharaman, K., Hausmann, B., Jungbluth, S.P., Kantor, R.S., Lavy, A., Warren, L.A., Rappé, M.S.,
307 Pester, M., Loy, A., and Thomas, B.C. (2018) Expanded diversity of microbial groups that shape the
308 dissimilatory sulfur cycle. *ISME J* **12**: 1715.

309 Ayers, M., Howell, P.L., and Burrows, L.L. (2010) Architecture of the type II secretion and type IV pilus
310 machineries. *Future Microbiol* **5**: 1203-1218.

311 Badalamenti, J.P., Summers, Z.M., Chan, C.H., Gralnick, J.A., and Bond, D.R. (2016) Isolation and
312 genomic characterization of 'Desulfuromonas soudanensis' WTL', a metal-and electrode-respiring
313 bacterium from anoxic deep subsurface brine. *Front Microbiol* **7**: 913.

314 Berry, J.-L., and Pelicic, V. (2015) Exceptionally widespread nanomachines composed of type IV pilins:
315 the prokaryotic Swiss Army knives. *FEMS Microbiol Rev* **39**: 134–154.

316 Bray, M.S., Wu, J., Reed, B.C., Kretz, C.B., Belli, K.M., Simister, R.L., Henny, C., Stewart, F.J.,
317 DiChristina, T.J., and Brandes, J.A. (2017) Shifting microbial communities sustain multi-year iron
318 reduction and methanogenesis in ferruginous sediment incubations. *Geobiology* **15**: 678-689.

319 Crowe, S.A., O'Neill, A.H., Kulczycki, E., Weisener, C.G., Roberts, J.A., and Fowle, D.A. (2007)
320 Reductive dissolution of trace metals from sediments. *Geomicrobiol J* **24**: 157-165.

321 Feliciano, G., Steidl, R., and Reguera, G. (2015) Structural and functional insights into the conductive pili
322 of *Geobacter sulfurreducens* revealed in molecular dynamics simulations. *Phys Chem Chem Phys* **17**:
323 22217-22226.

324 Filman, D.J., Marino, S.F., Ward, J.E., Yang, L., Mester, Z., Bullitt, E., Lovley, D.R., and Strauss, M.
325 (2019) Cryo-EM reveals the structural basis of long-range electron transport in a cytochrome-based
326 bacterial nanowire. *Comm Biol* **2**: 219.

327 Giltner, C.L., Nguyen, Y., and Burrows, L.L. (2012) Type IV pilin proteins: Versatile molecular modules.
328 *Microbiol Mol Biol Rev* **76**: 740-772.

329 Han, X., Kennan, R.M., Parker, D., Davies, J.K., and Rood, J.I. (2007) Type IV fimbrial biogenesis is
330 required for protease secretion and natural transformation in *Dichelobacter nodosus*. *J Bacteriol* **189**:
331 5022-5033.

332 He, S., Barco, R.A., Emerson, D., and Roden, E.E. (2017) Comparative genomic analysis of neutrophilic
333 iron (II) oxidizer genomes for candidate genes in extracellular electron transfer. *Front Microbiol* **8**: 1584.

334 Hernsdorf, A.W., Amano, Y., Miyakawa, K., Ise, K., Suzuki, Y., Anantharaman, K., Probst, A., Burstein,
335 D., Thomas, B.C., and Banfield, J.F. (2017) Potential for microbial H₂ and metal transformations
336 associated with novel bacteria and archaea in deep terrestrial subsurface sediments. *ISME J* **11**: 1915-
337 1929.

338 Holmes, D.E., Dang, Y., Walker, D.J., and Lovley, D.R. (2016) The electrically conductive pili of
339 *Geobacter* species are a recently evolved feature for extracellular electron transfer. *Microb Genom* **2**:
340 e000072.

341 Holmes, D.E., Shrestha, P.M., Walker, D.J., Dang, Y., Nevin, K.P., Woodard, T.L., and Lovley, D.R.
342 (2017) Metatranscriptomic evidence for direct interspecies electron transfer between *Geobacter* and
343 *Methanothrix* species in methanogenic rice paddy soils. *Appl Environ Microbiol* **83**: e00223-00217.

344 Hyatt, D., Chen, G.-L., LoCascio, P.F., Land, M.L., Larimer, F.W., and Hauser, L.J. (2010) Prodigal:
345 prokaryotic gene recognition and translation initiation site identification. *BMC Bioinformatics* **11**: 119.

346 Imam, S., Chen, Z., Roos, D.S., and Pohlschröder, M. (2011) Identification of surprisingly diverse type
347 IV pili, across a broad range of gram-positive bacteria. *PloS One* **6**: e28919.

348 Jones, D.T., Taylor, W.R., and Thornton, J.M. (1992) The rapid generation of mutation data matrices
349 from protein sequences. *Bioinformatics* **8**: 275-282.

350 Koch, C., and Harnisch, F. (2016) Is there a specific ecological niche for electroactive microorganisms?
351 *ChemElectroChem* **3**: 1282-1295.

352 Kolappan, S., Coureuil, M., Yu, X., Nassif, X., Egelman, E.H., and Craig, L. (2016) Structure of the
353 *Neisseria meningitidis* type IV pilus. *Nature Comm* **7**: 13015.

354 Kumar, S., Stecher, G., and Tamura, K. (2016) MEGA7: Molecular Evolutionary Genetics Analysis
355 version 7.0 for bigger datasets. *Mol Biol Evol* **33**: 1870-1874.

356 Leang, C., Qian, X., Mester, T., and Lovley, D.R. (2010) Alignment of the c-type cytochrome OmcS
357 along pili of *Geobacter sulfurreducens*. *Appl Environ Microbiol* **76**: 4080-4084.

358 Liu, X., Tremblay, P.-L., Malvankar, N.S., Nevin, K.P., Lovley, D.R., and Vargas, M. (2014) A
359 *Geobacter sulfurreducens* strain expressing *Pseudomonas aeruginosa* type IV pili localizes OmcS on pili
360 but is deficient in Fe (III) oxide reduction and current production. *Appl Environ Microbiol* **80**: 1219-1224.

361 Liu, X., Wang, S., Xu, A., Zhang, L., Liu, H., and Ma, L.Z. (2019) Biological synthesis of high-
362 conductive pili in aerobic bacterium *Pseudomonas aeruginosa*. *Appl Micro Biotechnol* **103**: 1535-1544.

363 Logan, B.E. (2009) Exoelectrogenic bacteria that power microbial fuel cells. *Nat Rev Microbiol* **7**: 375-
364 381.

365 Logan, B.E., Rossi, R., and Saikaly, P.E. (2019) Electroactive microorganisms in bioelectrochemical
366 systems. *Nat Rev Microbiol* **17**: 307-319.

367 Lovley, D.R. (1991) Dissimilatory Fe(III) and Mn(IV) reduction. *Microbiol Rev* **55**: 259-287.

368 Lovley, D.R. (2011) Live wires: direct extracellular electron exchange for bioenergy and the
369 bioremediation of energy-related contamination. *Energ Environ Sci* **4**: 4896-4906.

370 Lovley, D.R. (2017) Electrically conductive pili: biological function and potential applications in
371 electronics. *Curr Opin Electrochem* **4**: 190-198.

372 Lovley, D.R., and Coates, J.D. (1997) Bioremediation of metal contamination. *Curr Opin Biotechnol* **8**:
373 285-289.

374 Lovley, D.R., and Walker, D.J.F. (2019) *Geobacter* protein nanowires. *PeerJ Preprints* **7**: e27773v27771.

375 Mahadevan, R., Palsson, B.Ø., and Lovley, D.R. (2011) *In situ* to *in silico* and back: elucidating the
376 physiology and ecology of *Geobacter* spp. using genome-scale modelling. *Nat Rev Microbiol* **9**: 39-50.

377 Malvankar, N.S., Vargas, M., Nevin, K., Tremblay, P.-L., Evans-Lutterodt, K., Nykypanchuk, D., Martz,
378 E., Tuominen, M.T., and Lovley, D.R. (2015) Structural basis for metallic-like conductivity in microbial
379 nanowires. *mBio* **6**: e00084-00015.

380 Mehta, T., Childers, S.E., Glaven, R., Lovley, D.R., and Mester, T. (2006) A putative multicopper protein
381 secreted by an atypical type II secretion system involved in the reduction of insoluble electron acceptors
382 in *Geobacter sulfurreducens*. *Microbiology* **152**: 2257-2264.

383 Mikheenko, A., Saveliev, V., and Gurevich, A. (2015) MetaQUAST: evaluation of metagenome
384 assemblies. *Bioinformatics* **32**: 1088-1090.

385 Nguyen, Y., Sugiman-Marangos, S., Harvey, H., Bell, S.D., Charlton, C.L., Junop, M.S., and Burrows,
386 L.L. (2015) *Pseudomonas aeruginosa* minor pilins prime type IVa pilus assembly and promote surface
387 display of the PilY1 adhesin. *J Biol Chem* **290**: 601-611.

388 Nurk, S., Bankevich, A., Antipov, D., Gurevich, A.A., Korobeynikov, A., Lapidus, A., Prjibelski, A.D.,
389 Pyshkin, A., Sirokin, A., and Sirokin, Y. (2013) Assembling single-cell genomes and mini-
390 metagenomes from chimeric MDA products. *J Comp Biol* **20**: 714-737.

391 Probst, A.J., Ladd, B., Jarett, J.K., Geller-McGrath, D.E., Sieber, C.M., Emerson, J.B., Anantharaman, K.,
392 Thomas, B.C., Malmstrom, R.R., and Stieglmeier, M. (2018) Differential depth distribution of microbial
393 function and putative symbionts through sediment-hosted aquifers in the deep terrestrial subsurface.
394 *Nature Microbiol* **3**: 328-336.

395 Reardon, P.N., and Mueller, K.T. (2013) Structure of the type IVa major pilin from the electrically
396 conductive bacterial nanowires of *Geobacter sulfurreducens*. *J Biol Chem* **288**: 29260-29266.

397 Reguera, G., McCarthy, K.D., Mehta, T., Nicoll, J.S., Tuominen, M.T., and Lovley, D.R. (2005)
398 Extracellular electron transfer via microbial nanowires. *Nature* **435**: 1098-1101.

399 Reguera, G., Nevin, K.P., Nicoll, J.S., Covalla, S.F., Woodard, T.L., and Lovley, D.R. (2006) Biofilm and
400 nanowire production leads to increased current in *Geobacter sulfurreducens* fuel cells. *Appl Environ
401 Microbiol* **72**: 7345-7348.

402 Rotaru, A.-E., Shrestha, P.M., Liu, F., Markovaite, B., Chen, S., Nevin, K.P., and Lovley, D.R. (2014)
403 Direct interspecies electron transfer between *Geobacter metallireducens* and *Methanosaarcina barkeri*.
404 *Appl Environ Microbiol* **80**: 4599-4605.

405 Sydow, A., Krieg, T., Mayer, F., Schrader, J., and Holtmann, D. (2014) Electroactive bacteria—molecular
406 mechanisms and genetic tools. *Appl Micro Biotechnol* **98**: 8481-8495.

407 Szeinbaum, N., Nunn, B.L., Cavazos, A.R., Crowe, S.A., Stewart, F.J., DiChristina, T.J., Reinhard, C.T.,
408 and Glass, J.B. (2019) Expression of extracellular multiheme cytochromes discovered in a
409 betaproteobacterium during Mn(III) reduction. *BioRxiv*: 695007.

410 Tan, Y., Adhikari, R.Y., Malvankar, N.S., Ward, J.E., Woodard, T.L., Nevin, K.P., and Lovley, D.R.
411 (2017) Expressing the *Geobacter metallireducens* PilA in *Geobacter sulfurreducens* yields pili with
412 exceptional conductivity. *mBio* **8**: e02203-02216.

413 Tan, Y., Adhikari, R.Y., Malvankar, N.S., Ward, J.E., Nevin, K.P., Woodard, T.L., Smith, J.A.,
414 Snoeyenbos-West, O.L., Franks, A.E., and Tuominen, M.T. (2016) The low conductivity of *Geobacter*
415 *uranireducens* pili suggests a diversity of extracellular electron transfer mechanisms in the genus
416 *Geobacter*. *Front Microbiol* **7**: 980.

417 Vandecandelaere, I., Nercessian, O., Segaert, E., Achouak, W., Mollica, A., Faimali, M., De Vos, P., and
418 Vandamme, P. (2008) *Alteromonas genovensis* sp. nov., isolated from a marine electroactive biofilm and
419 emended description of *Alteromonas macleodii* Baumann et al. 1972 (Approved Lists 1980). *Int J Syst*
420 *Evol Microbiol* **58**: 2589-2596.

421 Vargas, M., Malvankar, N.S., Tremblay, P.-L., Leang, C., Smith, J.A., Patel, P., Snoeyenbos-West, O.,
422 Nevin, K.P., and Lovley, D.R. (2013) Aromatic amino acids required for pili conductivity and long-range
423 extracellular electron transport in *Geobacter sulfurreducens*. *mBio* **4**: e00105-00113.

424 Vuillemin, A., Friese, A., Alawi, M., Henny, C., Nomosatryo, S., Wagner, D., Crowe, S.A., and
425 Kallmeyer, J. (2016) Geomicrobiological features of ferruginous sediments from Lake Towuti, Indonesia.
426 *Front Microbiol* **7**: 1007.

427 Walker, D.J., Nevin, K.P., Holmes, D.E., Rotaru, A.-E., Ward, J.E., Woodard, T.L., Zhu, J., Ueki, T.,
428 Nonnenmann, S.S., and McInerney, M.J. (2019a) *Syntrophus* conductive pili demonstrate that common
429 hydrogen-donating syntrophs can have a direct electron transfer option. *BioRXiv*: 479683.

430 Walker, D.J.F., Martz, E., Holmes, D.E., Zhou, Z., Nonnenmann, S.S., and Lovley, D.R. (2019b) The
431 archaellum of *Methanospirillum hungatei* is electrically conductive. *mBio* **10**: e00579-00519.

432 Walker, D.J.F., Adhikari, R.Y., Holmes, D.E., Ward, J.E., Woodard, T.L., Nevin, K.P., and Lovley, D.R.
433 (2018) Electrically conductive pili from pilin genes of phylogenetically diverse microorganisms. *ISME J*
434 **12**: 48–58.

435 Wang, F., Gu, Y., O'Brien, J.P., Sophia, M.Y., Yalcin, S.E., Srikanth, V., Shen, C., Vu, D., Ing, N.L., and
436 Hochbaum, A.I. (2019) Structure of microbial nanowires reveals stacked hemes that transport electrons
437 over micrometers. *Cell* **177**: 361-369. e310.

438 Xiao, K., Malvankar, N.S., Shu, C., Martz, E., Lovley, D.R., and Sun, X. (2016) Low energy atomic
439 models suggesting a pilus structure that could account for electrical conductivity of *Geobacter*
440 *sulfurreducens* pili. *Sci Rep* **6**: 23385.

441